Bioactive Constituents of the Roots of *Licania intrapetiolaris*

Nicholas H. Oberlies,[†] Jason P. Burgess,[†] Hernán A. Navarro,[†] Rosa Elena Pinos,[‡] Djaja D. Soejarto,[§] Norman R. Farnsworth,[§] A. Douglas Kinghorn,[§] Mansukh C. Wani,*[,†] and Monroe E. Wall*[,†]

Chemistry and Life Sciences, Research Triangle Institute, P.O. Box 12194, Research Triangle Park, North Carolina 27709-2194, Facultad de Ciencas, Escuela Superior Politecnica de Chimborazo (ESPOCH), Riobamba, Ecuador, and Department of Medicinal Chemistry and Pharmacognosy, College of Pharmacy, University of Illinois at Chicago, Chicago, Illinois 60612

Received October 20, 2000

Fractionation of a methanol extract of the roots of *Licania intrapetiolaris*, as directed by activity against the KB assay, has led to the isolation of two novel clerodane diterpenoids, intrapetacins A (**1**) and B (**2**), and the known triterpenoid cucurbitacin B (**3**). The structures of **1** and **2** were deduced from one- and two-dimensional NMR experiments, including relative stereochemical assignments based on NOESY correlations and COSY coupling constants. Compound **3** was the most potent against the KB assay, but both **1** and **2** displayed moderate cytotoxicity. When evaluated against an antifungal assay using *Aspergillus niger*, **2** caused a significant zone of inhibition of fungal growth, while **1** was completely inactive. To the best of our knowledge, this is the first report of the isolation of bioactive compounds from the genus *Licania*.

In our collaborative program to search for novel antineoplastic agents from the Plant Kingdom, a methanol extract of the roots of *Licania intrapetiolaris* Spruce ex Hook (Chrysobalanaceae) showed promising bioactivity, as evaluated against the KB cytotoxicity assay. *L. intrapetiolaris* is a large tree that may grow up to 30 m in height and is widely distributed in tropical South America, including Columbia and Peru. Through the efforts of Morelli and co-workers, phytochemical investigations of *L. pittieri*,[1] *L. carii*,[2] *L. pyrifolia*,[3,4] and *L. heteromorpha*[5] have resulted in the isolation of several flavonoids, steroids, and triterpenoids, including four novel lupane derivatives.[4] However, to the best of our knowledge, no member of this genus has been subjected to a bioactivity-directed fractionation procedure previously. Therefore, we report herein the isolation and structure elucidation of three bioactive compounds from *L. intrapetiolaris*, namely, the novel clerodane diterpenoids, to which we have given the trivial names intrapetacin A (**1**) and B (**2**), and the triterpenoid cucurbitacin B (**3**).

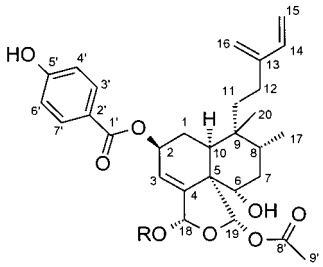

intrapetacin A (**1**) R=Me
intrapetacin B (**2**) R=Ac

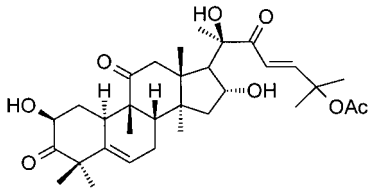

cucurbitacin B (**3**)

Results and Discussion

The KB cytotoxicity assay (see Experimental Section) was used at all steps of the fractionation process in order to concentrate the most cytotoxic principles from an extract of the roots of *L. intrapetiolaris*. Using a series of chromatographic techniques, including flash Si gel and RP-HPLC, the bioactive compounds intrapetacins A (**1**) and B (**2**) and cucurbitacin B (**3**) were isolated. Compounds **1** and **2** are new structures in a class of similar compounds that have been termed variously as either the clerodane diterpenoids,[6−17] the kolovane diterpenoids,[18] or the kolavene diterpenoids.[19] These have been isolated primarily from species of the genera *Casearia*,[6−9,12,13,15−19] *Laetia*,[14] and *Zuelania*[10,11] of the family Flacourtiaceae and have not been described previously from the Chrysobalanaceae; although Etse et al.[20] noted their presence in the Annonaceae. The triterpenoid cucurbitacin B (**3**) has been isolated from numerous genera,[17,21−24] although its existence in the genus *Licania* has been unreported until now.

Intrapetacin A (**1**) was isolated as an opaque amorphous solid and showed significant UV absorbance, especially near 254 nm, indicative of a conjugated π system. In the IR spectrum, diagnostic peaks were observed for hydroxyl (3581 cm^{-1}) and carbonyl (1746 and 1707 cm^{-1}) moieties. From the low-resolution ESIMS data, the molecular ion was observed via a Na^+ adduct at *m/z* 549 $[M + Na]^+$. Also, a major fragment peak, resulting from the loss of 60 amu (AcOH), was observed at *m/z* 489 $[M + Na - AcOH]^+$. The exact mass of the Na^+ adduct of the molecular ion, determined by HRFABMS, corresponded to a molecular formula of $C_{30}H_{38}O_8Na$ and an index of unsaturation of 12.

The complete ^1H, ^{13}C, and DEPT-135 NMR data for **1** are shown in Table 1. By comparing the ^{13}C and DEPT-135 NMR data, two terminal methylene units were recognized in the six-carbon side chain (C-11 through C-16). One of these, δ_H/δ_C 5.06, 5.23/112.66 (C-15), displayed classic[25]

* To whom correspondence should be addressed. Tel: 919-541-6440. Fax: 919-541-6499. E-mail: mcw@rti.org (M.C.W.) and jdr@rti.org (M.E.W.).
† Research Triangle Institute.
‡ Escuela Superior Politecnica de Chimborazo (ESPOCH).
§ University of Illinois at Chicago.

10.1021/np0005006 CCC: $20.00
Published on Web 04/12/2001

Table 1. ^{1}H NMR, ^{13}C NMR, and DEPT-135 Data for Compounds **1** and **2**

	intrapetacin A (**1**)			intrapetacin B (**2**)		
position	δ_C	DEPT	δ_H, multiplicity (J in Hz)	δ_C	DEPT	δ_H, multiplicity (J in Hz)
1eq/1ax	26.58	CH_2	2.32 m/1.78[a] m	26.46	CH_2	2.31 m/1.78[a] m
2	71.29	CH	5.80 m	71.02	CH	5.82 m
3	124.37	CH	6.11 brs	124.54	CH	6.03 brs
4	145.32	C		144.33	C	
5	53.61	C		53.68	C	
6	74.60	CH	4.04 dd (11.9, 3.9)	74.34	CH	4.07 dd (11.9, 3.8)
7	37.42	CH_2	1.89[a] m/1.69[a] m	37.40	CH_2	1.89[a] m/1.71[a] m
8	37.52	CH	1.78[a] m	37.55	CH	1.78 m[a]
9	38.16	C		38.18	C	
10	41.10	CH	2.42 dd (13.8, 2.9)	41.14	CH	2.43 dd (13.7 2.6)
11	27.66	CH_2	1.49[a] m/1.25[a] m	27.64	CH_2	1.51[a] m/1.23[a] m
12	23.74	CH_2	2.09 m	23.74	CH_2	2.06 m
13	145.24	C		145.06	C	
14	140.21	CH	6.44 dd (17.7, 11.2)	140.21	CH	6.44 dd (17.5, 10.8)
15	112.66	CH_2	5.23 d (17.7)/5.06 d (11.2)	112.64	CH_2	5.24 d (17.5)/5.05 d (10.8)
16	115.28	CH_2	5.04 s/4.94 s	115.35	CH_2	5.05 s/4.93 s
17	15.67	CH_3	0.93 d (6.5)	15.67	CH_3	0.94 d (6.7)
18	104.20	CH	5.48 m	95.17	CH	6.74 m
19	97.20	CH	6.43 s	97.53	CH	6.45 s
20	25.46	CH_3	0.97 s	25.42	CH_3	0.97 s
1′	166.03	C		166.08	C	
2′	122.43	C		122.27	C	
3′ and 7′	132.00	CH	7.96 d (9.0)	132.03	CH	7.96 d (8.4)
4′ and 6′	115.23	CH	6.87 d (9.0)	115.28	CH	6.87 d (8.4)
5′	160.29	C		160.29	C	
8′	170.34	C		169.90	C	
9′	21.59	CH_3	1.92[a] s	21.51	CH_3	1.92[a] s
10′	56.25	CH_3	3.43 s	170.18	C	
11′				21.18	CH_3	2.09[a] s
OH			5.89 brs			6.22 brs

[a] Assigned based on HMQC data.

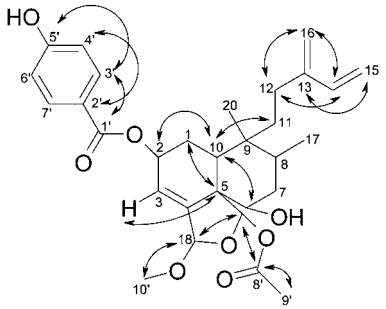

Figure 1. Selected HMBC correlations for intrapetacin A (**1**).

cis and *trans* coupling of 11.2 and 17.7 Hz, respectively, to δ_H/δ_C 6.44/140.21 (C-14). Conversely, the other terminal methylene, δ_H/δ_C 5.04, 4.94/115.28 (C-16), did not display any splitting, and thus, it was connected to a quaternary carbon, C-13. Furthermore, HMBC correlations (see Figure 1) between H-16 and C-14, and H-15 and C-13, placed these two ethylene units adjacent to each other. Also, position C-12 was determined to be adjacent to C-13 due to HMBC correlations between H-12 and C-14, H-14 and C-12, and H-16 and C-12. Position C-11 was then evident on the basis of COSY correlations between H-11 and H-12.

From the ^{1}H NMR spectrum of **1**, a *para*-substituted benzene ring was distinguished due to two well-separated doublets at δ_H 7.96 and 6.87, each with an integration equivalent to two protons and an *ortho* coupling constant of 9.0 Hz;[25] HMQC and DEPT-135 experiments correlated these to δ_C 132.00 (C-3′ and -7′) and 115.23 (C-4′ and -6′). The HMBC correlation (see Figure 1) between H-3′ and C-1′ indicated a linkage to an ester carbonyl, and the correlation of H-4′ to C-2′ established the point of attachment for this ester function. Also, the hydroxylated carbon was placed at C-5′ due to an HMBC correlation with H-3′. Beutler et al.[17] assigned the aromatic positions of a similar *p*-hydroxybenzoyl ester side chain in an alternative manner, wherein the chemical shifts for positions C-3′ and -7′ were interchanged with those for positions C-4′ and -6′. However, our assignments for this side chain were found to be in excellent agreement with classic calculations for ^{13}C NMR chemical shifts of substituted benzene rings.[25]

The characterization of the tricyclic core of the molecule of **1** was the most challenging aspect of the structure elucidation process. From the previous discussion, one ester, one benzene ring, and two exocyclic double bonds have been characterized, and these account for seven of the total 12 degrees of unsaturation. Also, from the ^{13}C NMR data, two of the remaining five degrees of unsaturation are due to an ester and a double bond. Hence, the extra degrees of unsaturation were presumed to be due to three rings.

Starting with the as-yet unassigned double bond between C-3 and C-4, COSY correlations were observed from H-3 to H-2 and, via weak allylic coupling, to H-18 (δ_H 5.48). A methoxy substituent (δ_H/δ_C 3.43/56.25, C-10′) was attached to C-18 (δ_C 104.20) due to HMBC correlations between H-10′ and C-18, and H-18 and C-10′. Moreover, a cyclic hemiacetal moiety was suggested between C-18 and C-19 (δ_H/δ_C 6.43/97.20) to account for the downfield chemical shift of both positions, and this was supported by HMBC correlations between H-18 and C-19, and H-19 and C-18. The low-resolution MS data indicated an acetate fragment, which was also evident in the NMR spectra (C-8′ and C-9′), and this was attached to C-19 by an HMBC correlation between H-19 and C-8′. COSY correlations were observed from H-2 to H-1, and H-1 to H-10. The quaternary bridge carbon, C-5 (δ_C 53.61), was determined on the basis of HMBC correlations from both H-1 to C-5 and H-3 to C-5; the chemical shift of the C-5 resonance is consistent with the literature values for similar clerodane diterpenoids.[17,18] The assignments to finalize the three-ring core of the

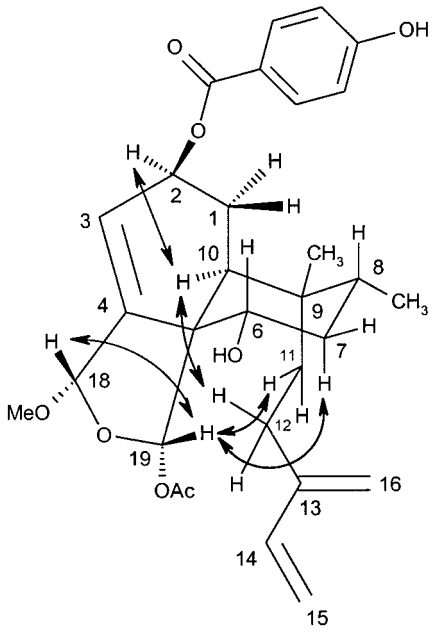

Figure 2. Selected NOESY correlations for intrapetacin A (**1**).

molecule were deduced from HMBC correlations between H-10 and C-6 and COSY correlations from H-6 to H-7.

To complete the structural assignment of **1**, the remaining ambiguities were the placement of the side chain units. The quaternary C-9 was determined to be the point of attachment both for the diene side chain (C-11 to C-16), due to HMBC interactions from H-11 to C-10, and for the uncoupled methyl, C-20. The other methyl group (H-17) displayed a doublet splitting pattern in the ^{1}H NMR spectrum with a *J* value of 6.5 Hz, and this was connected to H-8 via a COSY correlation. The chemical shift values of δ_H/δ_C 4.04/74.60 for position C-6 are consistent with typical chemical shifts for a hydroxyl-substituted methine group;[25] hence, the hydroxyl was placed at C-6 and the *p*-hydroxybenzoyl ester at C-2. In comparing compound **1** with other clerodane diterpenoids, nearly identical chemical shifts were observed by Chen and Wiemer[18] in the placement of a free hydroxyl at position C-6 and an acetate ester at position C-2 in compounds they termed corymobtins D and G.

Several unsuccessful attempts to crystallize **1** in a form suitable for X-ray crystallography necessitated the use of NMR coupling constants and NOESY data to assign the relative stereochemistry of the eight chiral centers. The *J* value of 13.8 Hz for the coupling of H-10 to H-1 indicated that H-10 is in an axial position.[25] A 1,3-diaxial NOESY correlation was observed between H-10 and H-2, which in turn placed the *p*-hydroxybenzoyl ester side chain in a pseudoequatorial position. The hydroxyl moiety attached to C-6 was assigned in an equatorial position, as there was diaxial coupling between H-6 and H-7 of 11.9 Hz. The splitting pattern of H-8 was complicated due to coupling with protons on H-7 and H-17. However, by homonuclear decoupling of the H-17 resonance, H-8 displayed a *J* value of 12.2 Hz, and thus, in a fashion similar to the H-6 assignment, H-8 was placed also in an axial position. A NOESY correlation between H-18 and H-19 placed these two protons in a *syn* relationship, and H-19 was configured as β due to NOESY correlations from H-19 to H-7 and H-11.[26] The relative stereochemistry was finalized via NOESY correlations between H-10 and H-12. The major NOESY interactions are illustrated in Figure 2, and the relative stereochemical assignments and optical rotation data (see Experimental Section) are consistent with the literature values for similar clerodane diterpenoids.[18] Beutler et al.[17] used X-ray crystallography data to assign the absolute stereochemistry for a series of clerodane diterpenoids that have a two-dimensional structure nearly identical to that of **1**. Those compounds, however, are enantiomeric with **1** in at least one position (C-2), and a comparison of the optical rotation data revealed values of approximately the same magnitude but with the opposite sign.[17]

Table 2. Cytotoxicity of Compounds **1**−**3** in the KB Assay

compound	EC_{50} value (μg/mL) ± SEM[a]
intrapetacin A (**1**)	2.0 ± 0.2
intrapetacin B (**2**)	0.8 ± 0.1
cucurbitacin B (**3**)	0.008 ± 0.002

[a] $n = 3$.

The IR and UV data for intrapetacin B (**2**) were nearly identical to that of **1** (see Experimental Section). However, in the low-resolution ESIMS, the molecular ion was observed via a Na^+ adduct ion at *m/z* 577 $[M + Na]^+$. Also, two fragments were observed, resulting from the loss of 60 amu (AcOH) at *m/z* 517 $[M + Na - AcOH]^+$ and 120 amu at *m/z* 457 $[M + Na - 2(AcOH)]^+$. The exact mass of the Na^+ adduct of the molecular ion, determined by HRFABMS, corresponded to a molecular formula of $C_{31}H_{38}O_9Na$ and an index of unsaturation of 13.

The complete ^{1}H, ^{13}C, and DEPT-135 NMR data for **2** are shown in Table 1. The entire data set is similar to that of **1** except for the addition of one acetate ester group (C-10′ and C-11′) and the absence of a methoxy group (position 10′ in **1**). In conjunction with a molecular weight difference between **1** and **2** of 28 amu (C═O), and an additional AcOH fragment in the low-resolution MS data, the conclusion was drawn that the methoxy moiety in **1** was replaced with an acetate ester substituent in **2**.

The COSY, HMQC, and HMBC experiments supported the same connectivity in **2** as in **1**. The second acetate ester side chain was connected to position 18 (δ_H/δ_C 6.74/95.17) due to an HMBC correlation from H-18 to C-10′. Furthermore, the ^{1}H and ^{13}C NMR chemical shift data in **2** for position 18 closely reflected the values observed for the other acetate-substituted hemiacetal, at position 19 (δ_H/δ_C 6.45/97.53). The NOESY and COSY correlations used to assign the relative stereochemistry of **1** were observed for **2** as well, and the specific rotation for **1** and **2** are of the same magnitude and in the same direction (see Experimental Section).

Finally, the triterpenoid cucurbitacin B (**3**) was isolated. The ^{13}C NMR data matched that published by Jacobs et al.,[23] and a standard sample of **3** was used to match the ^{1}H NMR data exactly.[22]

The EC_{50} values for **1**−**3** vs the KB assay are shown in Table 2, and it is apparent that **3** is the most potent of the compounds isolated from *L. intrapetiolaris*.[21,24] Beutler et al.[17] found cucurbitacins to be at least partially responsible for the cytotoxicity observed with an extract of *Casearia arborea* (L.C. Rich.) Urban (Flacourtiaceae), a plant that yielded clerodane diterpenoids of a structure very similar to **1** and **2**. The new clerodane diterpene compounds, **1** and **2**, described herein did display moderate activity vs KB as well. Furthermore, when examined in an antifungal assay (see Experimental Section), **2** induced a zone of inhibition of fungal growth of 21 mm, while **1** was completely inactive. This suggests that an acetate moiety at position 18 in **2** may impart more potent antifungal activity, or may protect the molecule from metabolic transformation more effectively, than the corresponding methoxy substituent in

1. In this same assay, a 0.01% solution of amphotericin B, a potent antifungal agent,[27] induced a zone of inhibition of approximately 18 mm.

Experimental Section

General Experimental Procedures. IR, UV, and specific rotation were recorded via a Nicolet Avatar 360 FT-IR, a Varian Cary 3 UV−vis spectrophotometer, and a Rudolph Autopol IV polarimeter, respectively. All NMR experiments were performed in $CDCl_3$ with TMS as an internal standard; COSY, NOESY, HMQC, HMBC, and ^{13}C and ^1H NMR spectra were run on a Bruker AMX-500 instrument, while a Bruker DPX-300 instrument was utilized for the DEPT-135 and ^{13}C NMR spectra. Low-resolution ESIMS were determined on a Finnigan LCQ with an electrospray interface; high-resolution FABMS were measured with a Micromass Autospec (Manchester, UK). Column chromatography was carried out on Si gel 60 (70−230 mesh, Merck, Darmstadt, Germany), and fractions were monitored via TLC (Si gel 60 F_{254} plates, 0.25 mm thickness) visualized with 5% phosphomolybdic acid in EtOH.

Plant Material. The root sample of *Licania intrapetiolaris* was collected in December of 1995, from a large tree of 30 m in height, 50 cm in diameter at breast height, growing in a tropical rain forest of Ecuador, within the Experimental Station of Escuela Superior Politecnica de Chimborazo (ESPOCH) in Los Vencedores (77° 56′ W longitude, 1° 30′ S latitude), Municipality of Puyo, Pastaza, at an altitude of about 900 m above sea level. Voucher herbarium specimens (Soejarto et al. 9400) have been deposited at the herbaria of ESPOCH (Riobamba, Ecuador) and the Field Museum of Natural History (Chicago, IL) under accession number 2161757.

Extraction and Isolation. The dried roots (525 g) were extracted initially with cold MeOH overnight (2 × 2L), followed by hot MeOH extraction in a Soxhlet (2 × 3 L) overnight; in each case the MeOH extracts were concentrated under reduced pressure. Separately, the extracts were partitioned first between 10% (aqueous) MeOH and hexane, and then the aqueous MeOH fraction was partitioned further between $CHCl_3$−MeOH (4:1) and H_2O. The organic layer was washed with 1% saline until there was no evidence of tannins.[28] The organic fraction from both the cold percolation and hot extraction had good bioactivity vs the KB assay, and each had a nearly identical TLC pattern; thus, they were combined to yield 2.9 g of material. This organic fraction was mixed with Celite and separated further on a flash Si gel column that was developed using a gradient of 1:1 hexane−$CHCl_3$ to 100% $CHCl_3$ to 20% MeOH. The fractions were combined into 14 pools on the basis of TLC properties and examined vs the KB assay. Pools 3 through 6 had promising activity and were combined (∼2 g), adsorbed onto Celite, and separated on a second flash Si gel column using a gradient of 100% hexane to 100% ethyl acetate to 25% MeOH. Again, fractions were pooled on the basis of TLC properties and tested vs the KB assay. Fraction 5 (∼550 mg), being the most potent, was purified via prep-scale RP-HPLC using a gradient of 6:4 MeOH−H_2O up to 100% MeOH on a C_8 column (21.4 mm i.d. × 250 mm). From the subsequent fractions, several repeated RP-HPLC separations, using similar solvent conditions on a C_{18} column (either 21.4 mm i.d or 10.0 mm i.d. × 250 mm), were used to isolate and purify compounds **1**−**3**. Compound **3** (35.4 mg; 0.0067%) was identified by direct comparison with an authentic sample[22] and by comparison (^{13}C NMR) with literature data.[23]

Intrapetacin A (1): 11.7 mg opaque amorphous solid, yield 0.0022% w/w; $[\alpha]^{19.1}_D$ −81.4° (*c* 0.28, $CHCl_3$); UV (MeOH) λ_{max} (log ϵ) 209 (4.43), 258 (4.32) nm; IR ($CHCl_3$) ν_{max} 3581, 3021, 2962, 2932, 1746, 1707, 1607, 1593, 1266, 1227, 1215, 1164, and 1110 cm^{-1}; ^1H NMR ($CDCl_3$, 500 MHz) and ^{13}C NMR ($CDCl_3$, 75 MHz) data, see Table 1; LRESIMS *m*/*z* 1075 $[2M + Na]^+$ (50), 549 $[M + Na]^+$ (98), 489 $[M + Na - AcOH]^+$ (23); HRFABMS *m*/*z* 549.2446 (calcd for $C_{30}H_{38}O_8Na$, 549.2464).

Intrapetacin B (2): 9.2 mg opaque amorphous solid, yield 0.0018% w/w; $[\alpha]^{19.7}_D$ −74.6° (*c* 0.19, $CHCl_3$); UV (MeOH) λ_{max} (log ϵ) 210 (4.47), 258 (4.35) nm; IR ($CHCl_3$) ν_{max} 3591, 3019, 2968, 2918, 1750, 1700, 1610, 1591, 1272, 1221, 1215, 1158, and 1100 cm^{-1}; ^1H NMR ($CDCl_3$, 500 MHz) and ^{13}C NMR ($CDCl_3$, 75 MHz) data, see Table 1; LRESIMS *m*/*z* 1131 $[2M + Na]^+$ (15), 577 $[M + Na]^+$ (98), 517 $[M + Na - AcOH]^+$ (27), 457 $[M + Na - 2(AcOH)]^+$ (6); HRFABMS *m*/*z* 577.2387 (calcd for $C_{31}H_{38}O_9Na$, 577.2414).

Cytotoxicity Assay. The KB (human oral epidermoid carcinoma) cytotoxicity assay was used to both monitor the fractionation process and measure the EC_{50} values for pure compounds. The assays were run in 96-well plastic plates, and each well contained 190 μL of a KB cell suspension (5×10^4 cells/mL) and 10 μL of the test material assayed in triplicate. For bioactivity-directed fractionation procedures, the fractions were assayed at 20 μg/mL, and any fraction that inhibited cell growth by >90% was considered to contain cytotoxic or "active" components and was subjected to further purification. For the EC_{50} calculations, pure compounds were assayed at 11 concentrations that ranged from 0.0025 to 20 μg/mL. Each plate also contained triplicate samples of vehicle (10% DMSO), and an 11-point camptothecin curve was used to monitor assay performance. The plates were incubated for 72 h before stopping the assay by the addition of 100 μL of 50% trichloroacetic acid. The relative amount of cell growth in each well was determined via a spectrophotometric assay as described previously.[29] The absorbance values were converted to percent survival using the formula $(Abs_{sample} - background)/(Abs_{vehicle} - background) \times 100$. The concentration of test compound that caused 50% cell death (EC_{50}) was determined from the semilog plot of percent survival vs log concentration fit to a sigmoid curve with variable slope using GraphPad Prism (v. 3.00 for Windows, GraphPad Software, San Diego, CA). These data are presented in Table 2 as the mean ± SEM.

Antifungal Assay. *Aspergillus niger* spores (kind gift of Professor Joseph O. Falkinham, III, Virginia Polytechnic Institute and State University) were diluted to 0.5 McFarland units in a buffered saline gelatin solution that contained 0.1 g of gelatin (Difco, Becton Dickinson Microbiology Systems, Sparks, MD), 8.5 g of NaCl, 0.3 g of KH_2PO_4, and 0.6 g of Na_2HPO_4 per liter of distilled H_2O. The spore suspension (100 μL) was added to 7.5 mL of warmed (∼45 °C) brain heart infusion broth (BHIB) that contained 3.7 g of brain heart infusion broth (Difco), 2.0 g of sucrose, and 12 g of agar (Difco) per liter. This agar preparation was then distributed evenly onto circular culture plates prefilled with 15 mL of BHIB and allowed to harden (∼5 min). Samples (10 μL of a 1.0% solution dissolved in 100% DMSO) were spotted onto the plates, wrapped in Parafilm, and incubated for 24 h at 30 °C. A vehicle control and a positive control, amphotericin B (0.01% solution; Sigma Chemical Co., St. Louis, MO), were run on each plate. Samples were considered active if they produced a measurable zone of inhibition. DMSO alone did not inhibit fungal growth, and 0.01% amphotericin B produced typically an 18 mm diameter zone of inhibition.

Acknowledgment. This research was supported by Grant U19-CA52956 from the National Cancer Institute, National Institutes of Health, Bethesda, MD. The collection and export of the plant sample were made as part of a collaborative research effort between ESPOCH and the University of Illinois at Chicago, under a Memorandum of Agreement signed by the two institutions in August 1995. We thank Dr. Jacinto C. Regalado, Jr., Field Museum of Natural History, Chicago, IL, for taxonomic assistance. High-resolution mass spectrometry data were acquired by the Nebraska Center for Mass Spectrometry in the Department of Chemistry at the University of Nebraska−Lincoln. The authors at Research Triangle Institute thank Elka Armstrong, Amanda Dew, Alison Keimowitz, Karol Parham, and Sharnelle Spaulding for technical assistance and Dr. Nam-Cheol Kim for his critique of the manuscript.

References and Notes

(1) Mendez, J.; Bilia, A. R.; Morelli, I. *Acta Pharm. Helv.* **1995**, *70*, 223−226.

(2) Bilia, A. R.; Mendez, J.; Morelli, I. *Acta Pharm. Helv.* **1996**, *71*, 191−197.
(3) Bilia, A. R.; Ciampi, L.; Mendez, J.; Morelli, I. *Acta Pharm. Helv.* **1996**, *71*, 199−204.
(4) Bilia, A. R.; Morelli, I.; Mendez, J. *J. Nat. Prod.* **1996**, *59*, 297−300.
(5) Braca, A.; De Tommasi, N.; Mendez, J.; Morelli, I. *Biochem. Syst. Ecol.* **1999**, *27*, 527−530.
(6) Itokawa, H.; Totsuka, N.; Takeya, K.; Watanabe, K.; Obata, E. *Chem. Pharm. Bull.* **1988**, *36*, 1585−1588.
(7) Itokawa, H.; Totsuka, N.; Morita, H.; Takeya, K.; Iitaka, Y.; Schenkel, E. P.; Motidome, M. *Chem. Pharm. Bull.* **1990**, *38*, 3384−3388.
(8) Morita, H.; Nakayama, M.; Kojima, H.; Takeya, K.; Itokawa, H.; Schenkel, E. P.; Motidome, M. *Chem. Pharm. Bull.* **1991**, *39*, 693−697.
(9) Itokawa, H.; Takeya, K. *Heterocycles* **1993**, *35*, 1467−1501.
(10) Khan, M. R.; Gray, G. I.; Reed, D. R.; Sadler, I. H.; Waterman, P. G. *Phytochemistry* **1990**, *29*, 1609−1614.
(11) Khan, M. R.; Gray, A. I.; Waterman, P. G. *Phytochemistry* **1990**, *29*, 2939−2942.
(12) Khan, M. R.; Gray, A. I.; Sadler, I. H.; Waterman, P. G. *Phytochemistry* **1990**, *29*, 3591−3595.
(13) Gibbons, S.; Gray, A. I.; Waterman, P. G. *Phytochemistry* **1996**, *41*, 565−570.
(14) Gibbons, S.; Gray, A. I.; Waterman, P. G. *Phytochemistry* **1996**, *43*, 635−638.
(15) Hunter, M. S.; Corley, D. G.; Carron, C. P.; Rowold, E.; Kilpatrick, B. F.; Durley, R. C. *J. Nat. Prod.* **1997**, *60*, 894−899.
(16) De Carvalho, P. R. F.; Furlan, M.; Young, M. C. M.; Kingston, D. G. I.; da S. Bolzani, V. *Phytochemistry* **1998**, *49*, 1659−1662.
(17) Beutler, J. A.; McCall, K. L.; Herbert, K.; Herald, D. L.; Pettit, G. R.; Johnson, T.; Shoemaker, R. H.; Boyd, M. R. *J. Nat. Prod.* **2000**, *63*, 657−661.
(18) Chen, T.-B.; Wiemer, D. F. *J. Nat. Prod.* **1991**, *54*, 1612−1618.
(19) Guittet, E.; Stoven, V.; Lallemand, J.-Y.; Ramiandrasoa, F.; Kunesch, G.; Moretti, C. *Tetrahedron* **1988**, *44*, 2893−2901.
(20) Etse, J. T.; Gray, A. I.; Thomas, D. W.; Waterman, P. G. *Phytochemistry* **1989**, *28*, 2489−2492.
(21) Cassady, J. M.; Suffness, M. In *Anticancer Agents Based on Natural Product Models*; Cassady, J. M., Douros, J. D., Eds.; Academic Press: New York, 1980; Chapter 7, pp 247−254.
(22) Che, C.-T.; Phoebe, C. H., Jr.; Kinghorn, A. D.; Farnsworth, N. R. *J. Nat. Prod.* **1985**, *48*, 429−434.
(23) Jacobs, H.; Singh, T.; Reynolds, W. F.; McLean, S. *J. Nat. Prod.* **1990**, *53*, 1600−1605.
(24) Fuller, R. W.; Cardellina, J. H., II; Cragg, G. M.; Boyd, M. R. *J. Nat. Prod.* **1994**, *57*, 1442−1445.
(25) Silverstein, R. M.; Bassler, G. C.; Morrill, T. C. *Spectrometric Identification of Organic Compounds*, 5th ed.; John Wiley & Sons: New York, 1991; pp 208, 221−222, and 239−241.
(26) Upon a reinspection of the NOESY data, the correlation between H-19 and H-7 was observed. To verify the relative stereochemical assignments before the final submission of the manuscript, **1** was examined in a ROESY experiment. The correlations observed in the earlier NOESY were seen as well in the ROESY.
(27) Jessup, C.; Reyes, G.; Fothergill, A.; McCarthy, D.; Rinaldi, M.; Messer, S.; Pfaller, M.; Ghannoum, M. *J. Chemother.* **2000**, *12*, 22−19.
(28) Wall, M. E.; Wani, M. C.; Brown, D. M.; Fullas, F.; Oswald, J. B.; Josephson, F. F.; Thornton, N. M.; Pezzuto, J. M.; Beecher, C. W. W.; Farnsworth, N. R.; Cordell, G. A.; Kinghorn, A. D. *Phytomedicine* **1996**, *3*, 281−285.
(29) Likhitwitayawuid, K.; Angerhofer, C. K.; Cordell, G. A.; Pezzuto, J. M.; Ruangrungsi, N. *J. Nat. Prod.* **1993**, *56*, 30−38.

NP0005006